Geomechanics and Engineering, *Vol. 30, No. 5 (2022) 449-460*
https://doi.org/10.12989/gae.2022.30.5.449

Probabilistic Q-system for rock classification considering shear wave propagation in jointed rock mass

Ji-Won Kim[1a], Song-Hun Chong[2b] and Gye-Chun Cho*[3]

[1]*Disposal Performance Demonstration Research Division, Korea Atomic Energy Research Institute, Daejeon 34057, Korea*
[2]*Department of Civil Engineering, Sunchon National University, 255 Jungang-ro, Sunchon, Jeollanam-do 57922, Korea*
[3]*Department of Civil and Environmental Engineering, KAIST, 291 Daehak-ro, Yuseong-gu, Daejeon 34141, Korea*

(*Received February 23, 2022, Revised June 20, 2022, Accepted August 13, 2022*)

Abstract. Safe underground construction in a rock mass requires adequate ground investigation and effective determination of rock conditions. The estimation of rock mass behavior is difficult, because rock masses are innately anisotropic and heterogeneous at different scales and are affected by various environmental factors. Quantitative rock mass classification systems, such as the Q-system and rock mass rating, are widely used for characterization and engineering design. The measurement of rock classification parameters is subjective and can vary among observers, resulting in questionable accuracy. Geophysical investigation methods, such as seismic surveys, have also been used for ground characterization. Torsional shear wave propagation characteristics in cylindrical rods are equal to that in an infinite media. A probabilistic quantitative relationship between the Q-value and shear wave velocity is thus investigated considering long-wavelength wave propagation in equivalent continuum jointed rock masses. Individual Q-system parameters are correlated with stress-dependent shear wave velocities in jointed rocks using experimental and numerical methods. The relationship between the Q-value and the shear wave velocity is normalized using a defined reference condition. This relationship is further improved using probabilistic analysis to remove unrealistic data and to suggest a range of Q-values for a given wave velocity. The proposed probabilistic Q-value estimation is then compared with field measurements and cross-hole seismic test data to verify its applicability.

Keywords: rock mass classification; Q-system; jointed rock mass; shear wave velocity; equivalent continuum

1. Introduction

Ground investigations and estimations of rock mass behavior are necessary for the safe and economical construction of underground structures (). Quantitative rock mass classification systems, such as the Q-system and rock mass rating, have been widely used to estimate rock mass behavior and deformability parameters (Barton *et al*. 1974, Bieniawski 1973, Bednarek and Majcherczyk 2020, Zhao *et al.* 2021, Zhou and Yang 2021). Rock mass classification systems organize rock masses into groups or classes of similar characteristics. This systematic identification and quantification can effectively predict rock mass behaviors and supply valuable engineering design assistance. The measurement of rock classification parameters is subjective and can vary from observer to observer, leading to questionable accuracy (Carter 2010, Edelbro *et al.* 2007). Rock masses are innately anisotropic and heterogeneous and contain discontinuities at different length scales, ranging in size from microcracks to faults. Thus, accurate estimation is problematic and affected by various factors, including confinement conditions, intact rock strength, joint wall roughness, joint filling materials, and weathering (Bandis *et al*. 1983).

Geophysical methods, such as seismic surveys, have been widely adopted in site characterization schemes to provide additional assistance for estimating rock mass behavior. Wave propagation in jointed rock masses is also affected by factors that influence rock classification systems. Hence, it is possible to estimate the variations in the rock mass classification values using wave velocity. The relationships between wave velocity and rock classification parameters (Sjøgren *et al*. 1979, Palmström 1996, El-Naqa 1996, Budetta *et al*. 2001, Isik *et al*. 2008, Bery and Rosli 2012) or classification values (Cha *et al*. 2006, Agliardi *et al*. 2016, Nourani *et al*. 2017, Kianpour *et al*. 2020) have been noted in previous studies from empirical and field test data. The estimation of rock modulus using small-strain compressional and shear wave velocities can overestimate the modulus values significantly for low-quality, highly jointed rock masses at shallow depths (Barton 2002). The wave velocity of jointed rock mass is lower than that of intact rock as the discontinuities cause wave attenuation. Jointed rocks are also more susceptible to changes in confining stress conditions due to the occurrence of stress-induced joint closure. Thus, the effects of stress-dependent rock joints must be considered in the relationship between rock mass classification and wave velocity.

Wave propagation in in-situ rock mass greatly depends

*Corresponding author, Professor
E-mail: gyechun@kaist.ac.kr
[a]Post-doctoral Researcher
E-mail: jwk@kaeri.re.kr
[b]Associate Professor
E-mail: shchong@scnu.ac.kr

ISSN: 2005-307X (Print), 2092-6219 (Online)

on the site conditions. Hence, a universal method that can accurately correlate the wave velocity with rock quality descriptors such as the Q-system for all site conditions is infeasible. Two rock zones with identical wave velocities can display drastically different characteristics during excavation (Barton 2006). However, geophysical wave velocity techniques can provide additional valuable insight and supplementary information for the evaluation rock mass modulus and strength.

Previous studies attempted to correlate electrical resistivity, another widely used geophysical survey method, with rock classification through theoretical relationships. Theoretical relationships between electrical resistivity and rock classification parameters were established to suggest a probabilistic relationship between electrical resistivity and rock classification values, such as the rock mass rating or Q-system (Ryu *et al*. 2013, Ryu *et al.* 2014, Hong *et al.* 2020). However, theoretical relationships for wave propagation in jointed rock mass focus on the wave propagation equations for individual or single set of joints (Cai and Zhao 2000, Zhao *et al*. 2008, Perino *et al*. 2010, Zhu *et al*. 2013, Li *et al*. 2014, Chai *et al*. 2016) and hence, lack the applicability to actual field situations where multiple joints are present. In addition, laboratory measurements of wave velocity differ from in-situ measurements as wave propagation greatly depends on the scale effects and specific site conditions. Therefore, a more appropriate method is needed to obtain a similar relationship between wave velocity and rock classification values considering actual wave propagation in in-situ rock mass.

In this study, a probabilistic relationship between the Q-value and shear wave velocity is investigated considering long-wavelength wave propagation in equivalent continuum jointed rock masses. The individual Q-system parameters are correlated with stress-dependent shear wave velocity measurements in jointed rocks via experimental and numerical studies. The relationships between the Q-system parameters and wave velocity are normalized using a reference jointed rock condition. The deduced relationship is improved through probabilistic filtering using a field dataset to remove low-probability cases. Verification of the quantitative relationship is conducted using cross-hole seismic-wave velocity data from a highway site in Korea. The Q-value estimations are then compared with on-site Q-value measurements to verify the applicability, reliability, and accuracy of the suggested relationship. It must be noted that the results of this study are not to suggest a new wave velocity-based classification system, but rather to provide a probabilistic estimation of rock mass classification when the conventional observations are impossible, such as during tunnel excavation.

2. Q-system and shear wave velocity

2.1 Long-wavelength wave propagation in jointed rock mass

The equivalent continuum model for wave propagation in jointed rocks ignores the effects of individual joints and considers the rock mass to be an equivalent continuum with a representative effective modulus. (Schoenberg and Muir 1989, Cook 1992, Li *et al*. 2010). This is analogous to long-wavelength propagation, where the wavelength of the propagating wave is much longer than the spatial heterogeneity of the rock mass. While the use of the equivalent continuum model can oversimplify the effects of rock joints on the rock mass properties and is nonapplicable when the joints are relatively large and sparsely spaced, it provides a simpler and accurate representation of in-situ rock mass where multiple joint sets are present.

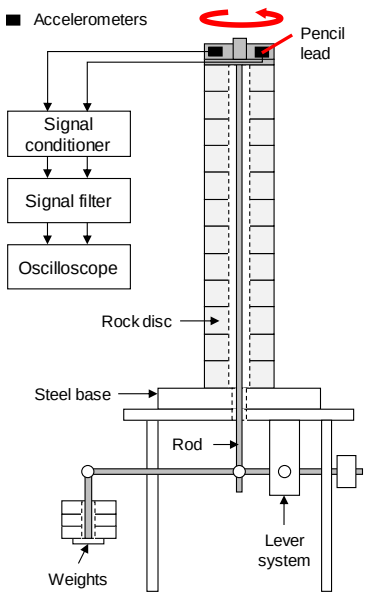

Fig. 1 Quasi-static resonant column test setup for long-wavelength shear wave velocity measurements (modified from Chong *et al*. 2020)

Based on the equivalent continuum model, the quasi-static resonant column (QSRC) test developed by Fratta and Santamarina (2002) can effectively measure the long-wavelength wave propagation in regularly spaced jointed rock column specimens as shown in Fig. 1. The QSRC test uses stacked rock discs to simulate an equivalent jointed rock mass having regularly spaced joints. More than 10 discs are required to allow long-wavelength propagation and prevent Brillouin dispersion (Cha *et al*. 2009). Quasi-static deformations below the elastic threshold level are applied to generate longitudinal and torsional excitations in jointed rock mass specimens and to measure the P- and S-wave velocities. Extensive studies on the effects of axial stress, material, two- and three-dimensional (2D and 3D, respectively) joint roughness, joint fill material, joint fill thickness, and joint cementation on elastic wave propagation in rock masses are performed using the QSRC setup (Fratta and Santamarina 2002, Cha *et al*. 2009, Mohd-Nordin *et al*. 2014, *Kim et al.* 2021). A numerical model for QSRC tests was also developed using the discrete element method program 3DEC and verified (Chong *et al*. 2020). A rock mass dynamic test was additionally developed to test the strain-dependent non-linear shear characteristics of equivalent jointed rock mass (Chong *et al.* 2014, Kim *et al.* 2018, Chong *et al.* 2021).

Table 1 Datasets used in this study

Data type (Reference)	Tested joint parameter	Related Q-system parameter	Tested rock conditions	Tested joint conditions
Experimental (Cha *et al.* 2009)	Joint fill material and thickness	Joint alteration number (J_a)	Gneiss rock discs 15 discs, 25.4 mm disc thickness Intact V_P=4,750 m/s Intact V_S=3,100 m/s	Stress: 37-445 kPa Sand fill: 0, 1.0, 1.5 mm Clay fill: 0, 0.5, 1.0, 1.5 mm
Experimental (Mohd-Nordin *et al.* 2014)	Joint roughness (3D)	Joint roughness number (J_r)	Dental gypsum discs* 12 discs, 30 mm disc thickness Intact V_P=3,845 m/s Intact V_S=2,450 m/s	Stress: 32-260 kPa Roughness (JRC): 0, 6-8, 12-14, 18-20
Numerical (This study)	Number of joint sets	Joint set number (J_n)	Gneiss rock discs 20 discs, 100 mm disc thickness Intact V_P=4750 m/s Intact V_S=3100 m/s	Stress: 37, 445 kPa Joint sets: 1, 2, 3, 4, 8
Theoretical (This study)	Number of joints	Rock quality designation (RQD)	-	Stress: 37, 445 kPa RQD: 10-100

Stress conditions: 37 and 445 kPa
Reference condition: planar joints (J_r=1), no joint fill (J_a=1), one joint set (J_n=2),<10 cm joint spacing (RQD=10, nominal value used)
Reference wave velocities: V_{S_37kPa}=573 m/s at 37 kPa, V_{S_445kPa}=1,027 m/s at 445 kPa
*Joint surface replicated from naturally fractured granite rock surfaces

For torsional shear waves in a cylindrical rod, the wave propagation characteristics are not affected by the geometry and are equal to the wave propagation characteristics in an infinite continuum (Kolsky 1963). The torsional shear waves are also non-dispersive when the cylindrical rod consists of a perfectly elastic material. Hence, assuming the equivalent continuum model, the jointed rock mass specimen adopted in the QSRC tests can be directly used to correlate the effects of joint conditions on shear wave propagation in the field.

2.2 Methodology for shear wave velocity-Q-system correlations

Experimental and numerical methods are used to determine the relationship between the individual Q-system parameters and the shear wave velocity based on the equivalent continuum model. The equivalent continuum jointed rock column with regularly spaced joints used in the QSRC tests are selected as the reference model for correlating the wave velocity of jointed rock masses and Q-system parameters. The experimental QSRC test datasets for different joint conditions from previous studies are used, as listed in Table 1. For each dataset, the wave velocity of the jointed rock column with a single set of clean-cut planar smooth joints and no joint fill is set as the reference condition. The change in wave velocity with respect to this reference condition is normalized with the reference wave velocity and used as a parametric factor that is later used for correlating the wave velocity and Q-value. Two reference stress conditions (37 and 445 kPa) are selected to investigate the effects of stress and represent near-surface and general stress conditions. The reference shear wave velocities are determined from a previous QSRC test using the same gneiss discs (Chong *et al*. 2020). The reference shear wave velocities are 573 m/s and 1,027 m/s for 37 and 445 kPa stress levels respectively. The intact shear wave velocity of the gneiss V_{S_intact} is 3,100 m/s.

The Q-system uses six basic parameters to classify and estimate rock characteristics: rock quality designation (RQD, rating: 0-100), joint set number (J_n, rating: 0.5-20), joint roughness number (J_r, rating: 0.5-4), joint alteration number (J_a, rating 0.75-20), joint water reduction number (J_w, 0.05-1), and stress reduction factor (SRF, 1-400). The shear wave velocity of rock masses is correlated with the RQD, J_n, J_r, and J_a parameters, which are causally related to the properties of the rock mass and rock joints. The environmental factors, J_w and SRF, are assumed for general dry or minor inflow (J_w=1) and favorable stress (SRF=1) conditions. The relationships between wave velocity and the site-dependent environmental factors are neglected in this study. The relationship between wave velocity and each Q-system classification parameter is deduced using the following steps:

(1) The QSRC test data consists of shear wave velocity values at each axial stress level for a given joint condition. The data is modified such that the wave velocity is plotted with the respective Q-system classification parameter value for each tested joint condition at 37 kPa and 445 kPa axial stress
(2) The shear wave velocity and Q-system classification parameter values are normalized by the wave velocity and classification parameters values of the reference condition
(3) Interpolation is used to calculate the normalized wave velocity data for any missing Q-system classification parameter values

It is noted that the individual classification parameters are not independent and depend on one another when computing the Q-value of a rock mass in a realistic scenario. To compensate for this, field data is used to filter the correlations to provide a more probable relationship between wave velocity and Q-value.

For the relationship between wave velocity and the joint set number J_n that could not be tested experimentally, discrete element numerical analysis using the 3D distinct

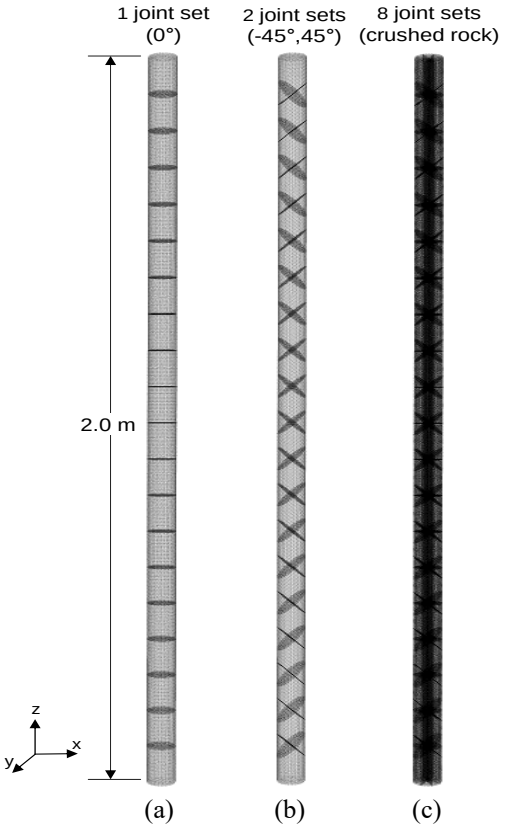

Fig. 2 3D model for number of joint sets. (a) joint locations of reference QSRC test specimen (equally spaced planar joints, 1 joint set, 0° orientation); (b) simulated jointed rock specimen (two joint sets, -45 and 45° orientations, J_n=4); and (c) simulated crushed rock specimen (eight joint sets, J_n=20)

element code (3DEC, Itasca 2013) was performed. The discrete element method is widely used in rock mechanics because of its ability to model the discrete and discontinuous characteristics of rock masses. Based on the preliminary numerical model for simulation of QSRC tests outlined in Chong *et al.* (2020), the cylindrical jointed rock specimens used in the QSRC tests are replicated in the 3DEC to perform numerical experiments. The rock quality designation parameter is also correlated with the wave velocity by assuming and ideal rock core and using a Wyllie time-average equation.

3. Numerical study

3.1 Effect of number of joint sets

The effects of the joint set number on the wave velocity are numerically examined, owing to the physical difficulties in specimen preparation. A 2-m tall cylindrical rock specimen having 19 evenly spaced clean-cut joints perpendicular to the specimen axis (0°) is modeled, as shown in Fig. 2. The model replicates a QSRC specimen with 20 rock discs of 100-mm thickness that fits the long-wavelength assumption. The mesh size is set to 0.01 m to obtain optimum numerical

Table 2 Rock material and joint properties used in numerical analysis

Gneiss disc properties	
Dimensions	Inner diameter=25 mm Outer diameter=63 mm Specimen length=1,000 mm
Material properties(1)	Density ρ=2,704 kg/m^3 Bulk modulus K=26.4 GPa Shear modulus G=26.0 GPa
Rock joint interface properties	
Joint model	Elastic joint model (no slip or joint failure)
Joint stiffness properties(1)	37 kPa Shear k_{s_37kPa}=36.7 GPa/m 445 kPa Shear stiffness k_{s_445kPa}=127.7 GPa/m
Test parameters	
Number of joint sets	1, 2, 3, 4, 8 joint sets (Corresponding to J_n=0.5, 2, 4, 9, 15, 20) Joint set angles: -45, 0, 45° with respect to the horizontal x-y plane

(1) Material and joint properties of rock obtained from previous numerical studies outlined in Chong *et al.* (2020).

stability and satisfy the Courant number for the given model dimensions (Robertsson *et al.* 1994, Zerwer *et al.* 2002). The elastic joint model is assigned to the joints to replicate the elastic joint deformation characteristics. Stress boundaries are applied at the top of the specimen to replicate the axial loading in the QSRC tests. The bottom boundary is fixed to simulate the necessary fixed-free boundary conditions. The rock material and joint properties used in the numerical analysis are listed in Table 2.

The different joint set numbers and orientations are simulated by adding joint sets to the same joint location with different joint orientations (-45, 0, and 45° with reference to the horizontal x-y plane). This enables all other joint sets to have identical joint spacings and follows the equivalent continuum assumption. The multiple joint orientations can account for the effects of different joint orientations present in rock mass, as inclined joints display increased joint stiffness in a jointed rock column specimen (Sebastian and Sitharam 2018). It is noted that while the selected joint orientations are an idealized representation of the joint set number and may not portray the actual effects of number of joint sets in in-situ rock masses, it is suitable for computing a probable representative wave velocity value for the given joint set number. The velocities obtained from each joint orientation combination were averaged to determine the representative wave velocity for each joint set number value. Eight joint sets were used to simulate the crushed rock via systematic addition, as shown in Fig. 2(c). The normal and shear joint stiffnesses obtained from QSRC tests on gneiss rock discs with smooth, clean-cut joints at 37 kPa and 445 kPa axial stresses are input as joint properties. A summary of the numerical test cases is presented in Table 3.

3.2 Relationship between J_n and shear wave velocity

The shear wave velocities for different joint set numbers obtained from the numerical analysis are shown in

Table 3 Summary of numerical test cases

Joint set condition	J_n value	Number of joint sets	Joint set angle combinations
Massive, no or few joints	0.5-1 (set as 0.5)	0	1 (none, intact)
One joint set	2	1	3 (-45°/ 0°/ 45°)
Two joint sets	4	2	3 (0°,-45°/ 0°,45°/-45°,45°)
Three joint sets	9	3	1 (-45°, 0°, 45°)
Four or more joint sets, heavily jointed	15	4	1 (-45°, 0°, 45°, vertical joint)
Crushed rock, earthlike	20	8	1 (-45°, 0°, 45°, random joints)

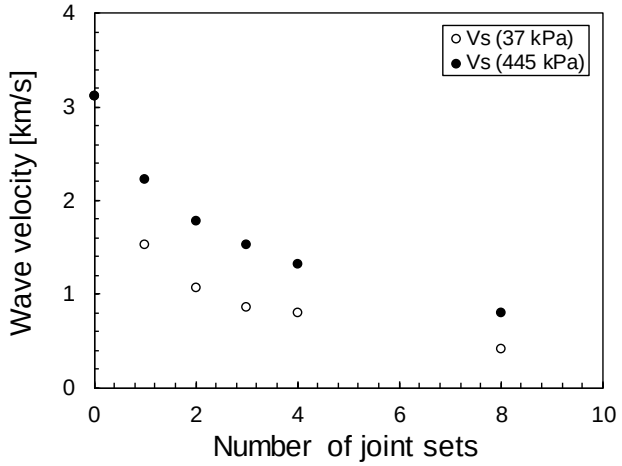

Fig. 3 Shear wave velocities at 37 kPa and 445 kPa axial stress for different number of jointed sets

Fig. 3. The shear wave velocities decrease for both axial stress levels with an increased joint set number. The increased joint set number provides more sources of stiffness reduction in the jointed rock specimen. Larger shear wave velocities are observed at 445 kPa axial stress as increased confinement and joint stiffness improved wave propagation.

The shear wave velocity data are correlated with the Q-system J_n parameter. First, a power function is used to correlate the wave velocities with the six J_n rating values considered in the numerical analysis (J_n=0.5, 2, 4, 9, 15, 20) as shown in Fig. 4(a). Based on this trend, the missing wave velocities for the remaining J_n values (J_n=1, 3, 6, 12) are interpolated. Using the interpolated shear wave velocities obtained from the trendline, the wave velocities were normalized using the shear wave velocity corresponding to J_n=2 (the defined reference condition of one joint set), as shown in Fig. 4(b). The joint set number factor, *fJN*, is defined as the shear wave velocity value corresponding to each J_n rating normalized by the reference shear wave velocity.

4. Relationship between Q-system parameters and wave velocity from QSRC test

4.1 Relationship between RQD and shear wave velocity

The *RQD* is defined as the percentage length of core pieces longer than 10 cm in a recovered core (Deere, 1963). Previous studies have noted a general increase in in-situ wave velocity with increased *RQD* (Leucci and De Giorgi 2006, Bery and Rosli 2012, Salaamah *et al*. 2018). A given rock core will have pieces either longer or smaller than the 10 cm threshold. Assuming that a core is comprised of two distinct components, an intact rock component and a jointed rock component, we can assume a Wyllie time-average equation for the shear wave velocity V_S of a given *RQD* value is as follows (Wyllie *et al.* 1958)

$$V_S = \left(\frac{\left(\frac{RQD}{100}\right)}{V_{Si}} + \frac{\left(1-\frac{RQD}{100}\right)}{V_{Sj}} \right)^{-1}, \quad (1)$$

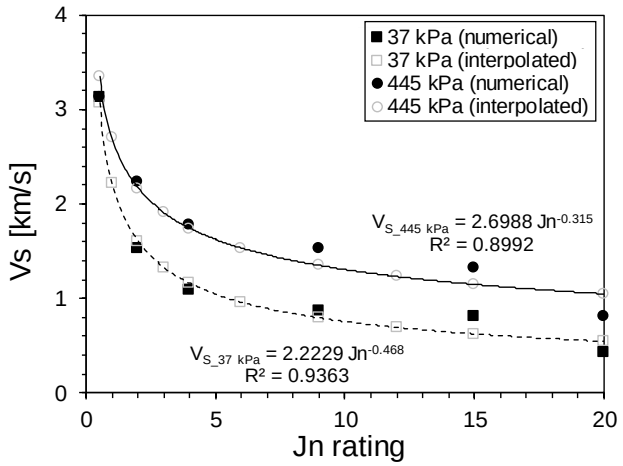

(a) Interpolation of missing shear wave velocities

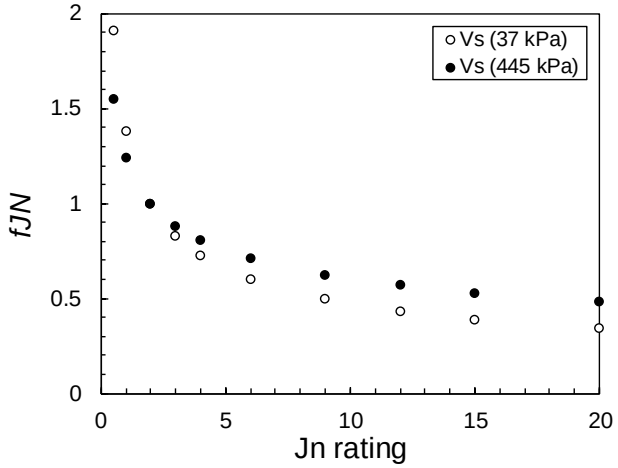

(b) Relationship between J_n rating and normalized shear wave velocity (Joint set number factor *fJN)*

Fig. 4 Process for calculating the joint set number factor *fJN*

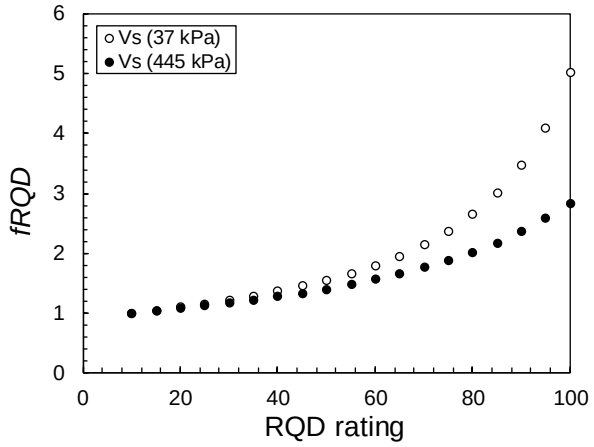

Fig. 5 Relationship between *RQD* rating and normalized shear wave velocity (*RQD* factor *fRQD*)

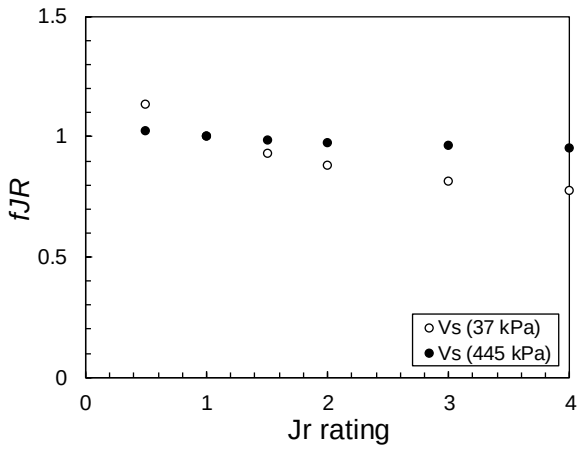

Fig. 6 Relationship between J_r rating and normalized wave velocity (Joint roughness factor *fJR*)

where V_{Si} is the shear wave velocity of the intact rock determined from laboratory tests (e.g., ultrasonic and impact echo tests), and V_{Sj} is the shear wave velocity of the jointed rock mass determined from QSRC tests. From Eq. (1), the shear wave velocity increases with increasing *RQD* as the intact rock component of the core increases. The reference shear wave velocities for 37 and 445 kPa stress levels are determined from QSRC tests on rock specimens with a joint spacing of 25 mm (*RQD*=0). Hence, a nominal *RQD* value of 10 is used to evaluate the Q-value (NGI 2013). The shear wave velocity corresponding to *RQD*=10 is used to normalize the wave velocity data. The rock quality designation factor, *fRQD*, shown in Fig. 5. is defined as the shear wave velocity values that correspond to each *RQD* rating normalized by the reference shear wave velocity.

4.2 Relationship between J_r and shear wave velocity

The joint roughness number J_r is related to the rock-wall contacts and the length scale of the rock asperities. The relationship between J_r and the shear wave velocity is obtained from previous QSRC test data. Cha *et al.* (2009) tested 2D roughness profiles and found that well-matched surfaces contributed to improved wave propagation. Mohd-Nordin *et al.* (2014) tested natural 3D roughness profiles and found that the longitudinal wave velocities increased with increased joint roughness, owing to the enhanced contact area. Meanwhile, the shear wave velocities decreased with increased joint roughness as the joint roughness increased interlocking and shear resistances. Increased joint roughness thus leads to improved surface contact at lower stresses (Kahraman 2002). However, the joint roughness in the field largely depends on the scale at which the roughness exists and the given stress conditions. The effects of joint roughness also greatly depend on the joint infill. If the joint infill material prevents rock wall contact, the roughness is no longer significant and the properties of the infill material is dominant.

The relationship between J_r and the shear wave velocity is obtained from the QSRC test data outlined by Mohd-Nordin *et al.* (2014). The shear wave velocities corresponding to different joint roughness coefficient (JRC) ranges are adapted and fitted to different J_r rating values. The relationship between JRC and J_r suggested by Barton (1987) for 200 mm and 1,000 mm profile samples display a general increase in J_r with increased JRC. While the effects of joint roughness are highly dependent on the spatial scale of the asperities with respect to the size of the rock mass, the correlations between JRC and J_r are assumed for the size of the jointed rock column specimen. The higher JRC values from the test data is assumed to correspond to the rough, irregular, and discontinuous joints, and the lower JRC values correspond to smooth or slickenside planar joints. Because the range of axial stress is limited to 260 kPa in the dataset, the wave velocity-stress trendlines are extrapolated for shear wave velocities at 445 kPa. The missing shear wave velocities for the remaining J_r values (J_r=1.5,3) are interpolated using wave velocity-stress trendlines. For the defined reference condition of smooth planar joints, the shear wave velocities corresponding to J_r=1 are used to normalize the shear wave velocity data, as shown in Fig. 6. The joint roughness factor, *fJR*, is defined as the shear wave velocity values corresponding to each J_r rating normalized by the reference shear wave velocity. Note that only small changes in *fJR* occur with changes in joint roughness, reinforcing the notion that J_r seems irrelevant for connections between rock mass quality and seismic velocities (Barton 2002).

4.3 Relationship between J_a and shear wave velocity

The joint alteration number, J_a, is related to the type of gouge fill material and its fill thickness. The relationship between J_a and shear wave velocity is obtained from previous studies on the QSRC test. Fratta and Santamarina (2002) tested clay-filled joints having thicknesses up to 2.5 mm and found that clay adds significant loss to wave propagation, leading to decreased shear wave velocity and increased damping with increased joint fill thickness. Cha *et al.* (2009) tested sand- and clay-filled joints ranging from 0.5 to 1.5 mm and noted similar reductions in wave velocity and damping. Thicker joint fills resulted in lower initial stiffness and lower seismic wave transmission across the

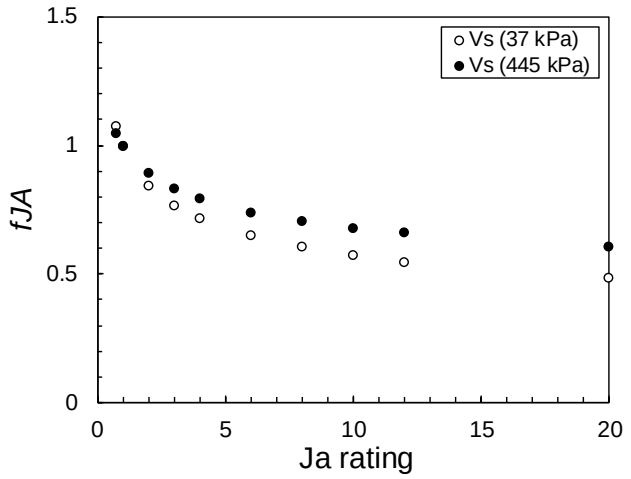

Fig. 7 Relationship between J_a rating and normalized wave velocity (Joint alteration factor *fJA*)

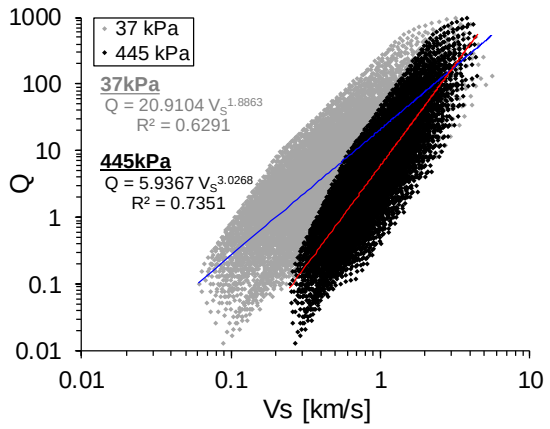

Fig. 8 Relationship between shear wave velocity and Q-value for 37 kPa and 445 kPa axial stress. Each point represents a unique combination of *fRQD*, *fJN*, *fJR* and *fJA*

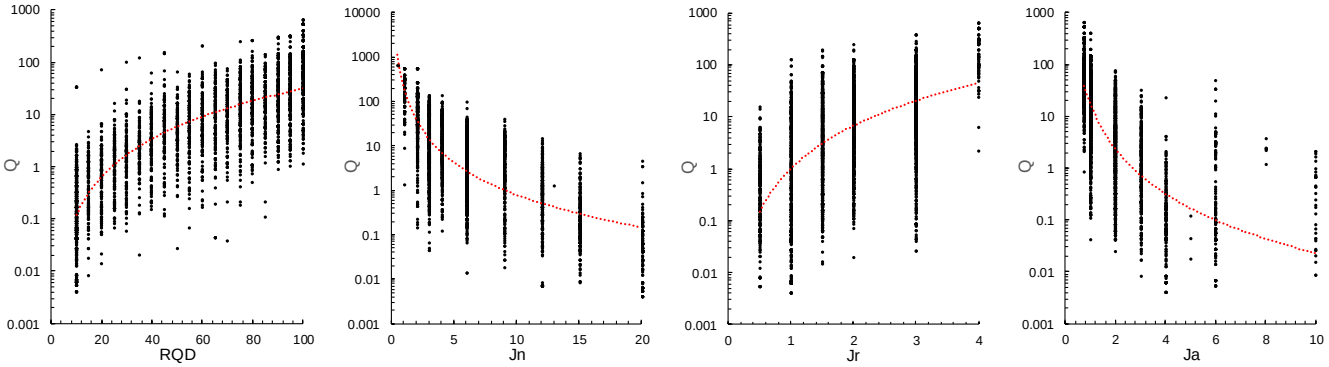

(a) *RQD* (b) J_n (c) J_r (d) J_a

Fig. 9 Relationship between Q-system classification parameters and Q-value for the field dataset

fractures (Gong *et al.* 2018).

The relationship between J_a and the shear wave velocity is then obtained from the QSRC test data outlined by Cha *et al.* (2009). The shear wave velocities corresponding to sand-and clay-filled joints are adapted and fitted to different J_a rating values. No joint fills correspond to fresh wall joints (J_a=1), thin fillings of 1-mm thickness correspond to think fillings having some rock-wall contact (J_a=3 for sand, J_a=4 for clay) and those of 1.5-mm thickness correspond to thick fillings having no wall contacts (J_a=8 for sand, J_a=12 for clay). Based on the wave velocity-stress trendlines, the missing shear wave velocities for the remaining J_a values (J_a=0.75, 2, 6, 10, 20) are interpolated. For the defined reference condition of no joint fill, the shear wave velocities corresponding to J_a=1 are used to normalize the shear wave velocity data, as shown in Fig. 7. The joint alteration factor, *fJA*, is defined as the shear wave velocity values that correspond to each J_a rating normalized by the reference shear wave velocity.

5. Probabilistic correlation between Q-system and shear wave velocity

5.1 Relationship between Q-system and shear wave velocity

The relationship between the Q-value and shear wave velocity is obtained from the relationships between the individual Q-system parameters and shear wave velocity. Based on the parametric factors, *fRQD*, *fJN*, *fJR*, and *fJA*, the Q-system equations for the P- and S-wave velocities can be derived as follows

$$V_Q = V_{ref} \times fRQD \times fJR \times fJN \times fJA, \quad (2)$$

where V_Q is the calculated shear wave velocity according to the reference value, V_{ref} is the shear wave velocity for the reference conditions, and *fRQD*, *fJN*, *fJR*, and *fJA* are the factors for each Q-system parameter. The deduced relationship between the Q-value and shear wave velocity is shown in Fig. 8. Each point on the scatter plot corresponds to a unique combination of *fRQD*, *fJN*, *fJR*, and *fJA*. The Q-value increases with increasing shear wave velocity, and larger gradients are displayed for higher stress levels. However, the relationships contain all combinations of Q-system parameter factors and exhibit a wide range of scatter. An example shear wave velocity of 1 km/s yields a Q-value range of 1-280 for 37 kPa and 0.3-50 for 445 kPa. The relationship covers an extensive range of Q-values for a single shear wave velocity value and hence, is not meaningful for determining accurate rock mass conditions.

Table 4 Removal criteria and correlation coefficients

Category	R_{at} criteria	R_{ap} criteria	Pearson correlation coefficient	
			V_S at 37 kPa	V_S at 445 kPa
Original	0	0	0.7932	0.8574
Case 1	<0.005	<0.05	0.9084	0.9340
Case 2	<0.010	<0.10	0.9256	0.9487
Case 3	<0.015	<0.15	0.9653	0.9779

5.2 Probabilistic data reduction

The particular combinations of Q-system factors in Fig. 8 are improbable (e.g., jointed rock mass with an *RQD* rating of 100 with a simultaneous joint set number of 20 (crushed rock)). Hence, attempts have been made to reduce data scattering through a probabilistic approach using actual field data. A dataset of 4,698 Q-values and respective Q-system parameters from nine railway and road construction sites in Korea are used in this study. The field dataset shown in Fig. 9 displays an increase in Q-value with increased *RQD* and J_r, and a decrease in Q-value with increased J_n and J_a. These correlations are similar to the relationships between Q-system parameters and shear wave velocity obtained from the QSRC test data. As noted earlier, J_r has less influence compared to the other classification parameters in the relationship between rock mass quality and seismic velocity. The unrealistic relationships are filtered and removed by examining the combinations of the two Q-system parameters. First, the probability, R_{at}, of a specific combination of two Q-system parameter values existing in the total dataset is examined (e.g., 97 values in the dataset are both *RQD*=75% and J_n=3, then R_{at}=97/4,689=0.0207). Second, the probability R_{ap} of one parameter existing with respect to the other parameter in that specific combination is examined (for example, 212 values in the dataset are *RQD*=75%, then R_{ap}=97/212=0.457. The 1,229 values in the dataset are J_n=3, and R_{ap}=97/1,229=0.079). This data filtering process is similar to the process adopted for the probabilistic relationship between electrical resistivity and Q-value (Ryu *et al*. 2013, Hong *et al.* 2020).

The three criteria of R_{at} and R_{ap} values used to remove the less probable combinations and their respective coefficients of determination are listed in Table 4. The relationship between the Q-value and shear wave velocity after the application of each removal criterion is shown in Fig. 10. The relationship between Q-value and shear wave velocity improved with stricter filtering, resulting in less data scatter and a more visible trend. The Pearson correlation coefficient increases for both stress levels with stricter filtering criterion and progressive removal of data points. While the probabilistic data removal provides a less scattered log-log linear correlation between the shear wave velocity and Q-value, a certain degree of data scatter still remains. Hence, a confidence ellipse is adopted to provide a range of Q-values for each given shear wave velocity, rather than a single Q-value. The 80%, 95% and 99.9% confidence ellipse for the Q-value-shear wave velocity relationship after the application of the case 3 removal criteria (R_{at}<0.015, R_{ap}<0.05) is drawn in the log-log scale, as

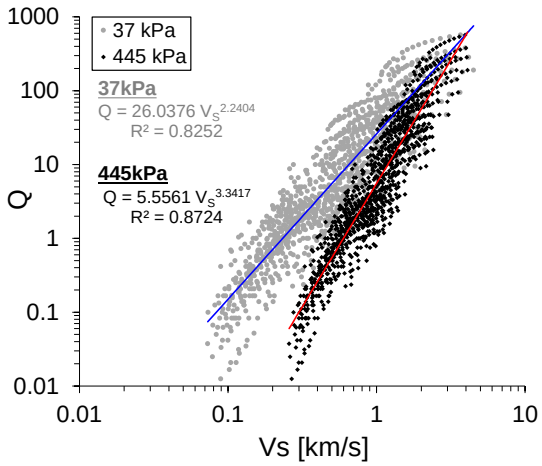

(a) Case 1 (R_{at}<0.005, R_{ap}<0.05)

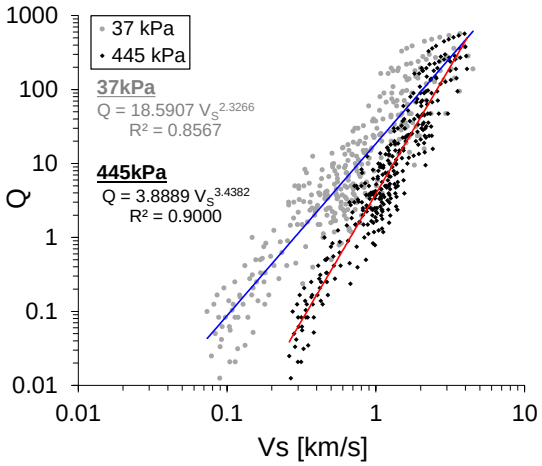

(b) Case 2 (R_{at}<0.010, R_{ap}<0.10)

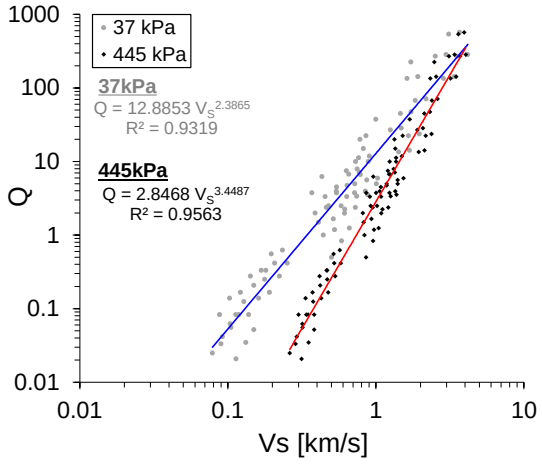

(c) Case 3 (R_{at}<0.015, R_{ap}<0.15)

Fig. 10 Probabilistic relationship between Q-value and shear wave velocity for each removal criteria

shown in Fig. 11. The ellipse can be used to provide a range of probabilistic Q-values for a given shear wave velocity. For example, a shear wave velocity of 2 km/s results in a 95% confidence Q-value range of 11-255 for 37 kPa and 6-95 for 445 kPa. Without the error ellipses, the 2 km/s shear wave velocity will result in a single Q-value of 53 for 37 kPa and 23 for 445 kPa.

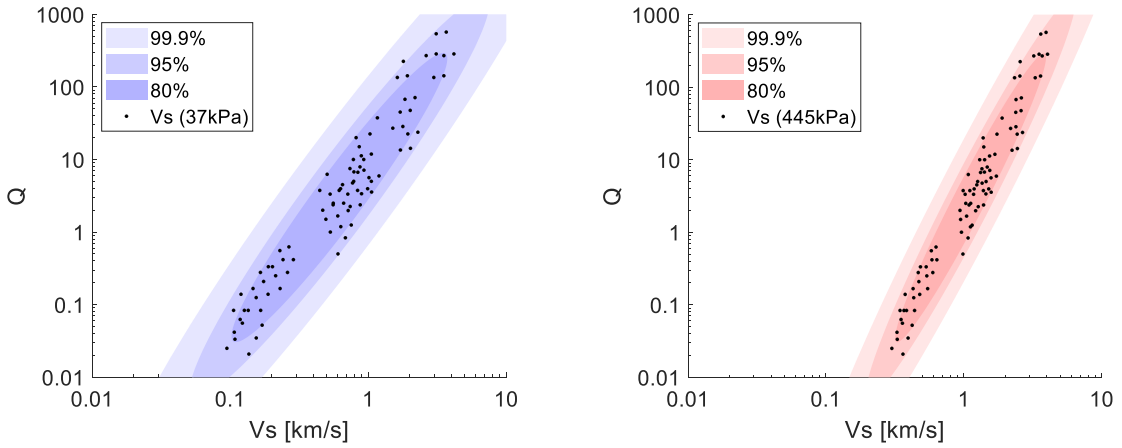

(a) 37 kPa stress level (b) 445 kPa stress level

Fig. 11 Confidence ellipses for RMR-shear wave velocity relationships from the Case 3 removal criteria

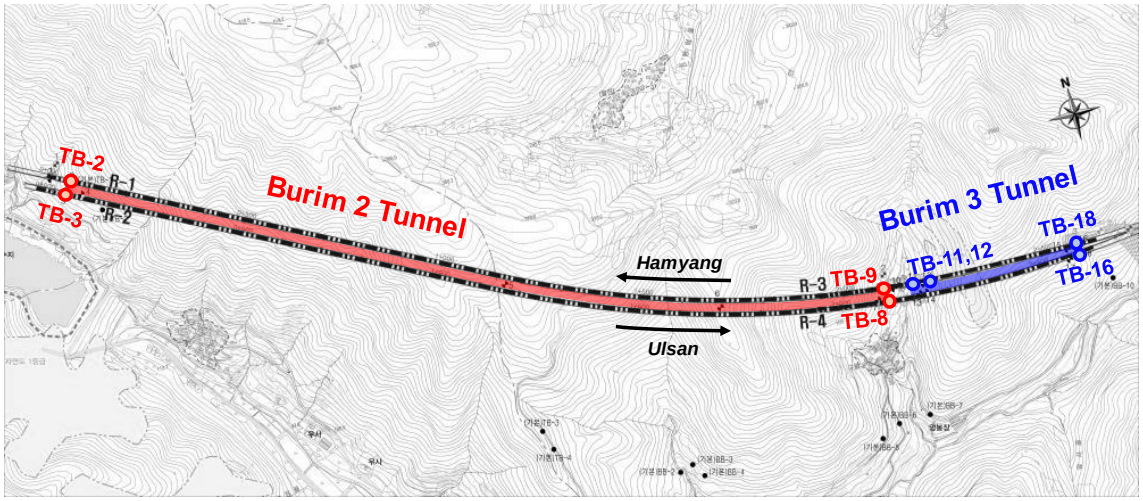

Tunnel section	Start of Burim 2	End of Burim 2/Start of Burim 3	End of Burim 3
	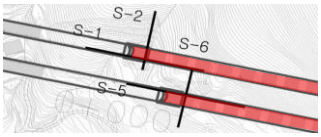	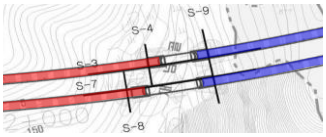	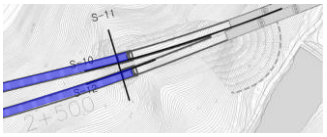
Depth of soil layer (m) (velocity<1.6 km/s)	0.1-9.7	0.0-5.4	0.6-5.3
Depth of rock layer (m) (velocity 1.6-2.8 km/s)	3.0-12.5	1.2-11.3	1.3-13.6

Fig. 12 Site features of the Burim 2 and Burim 3 tunnel sections of the Hamyang-Ulsan Expressway

6. Application of the Q-value-shear wave velocity relationships

The Q-value-shear wave velocity relationships are verified through cross-hole seismic-wave velocity data from the Burim 2 and Burim 3 tunnel sections of the Hamyang-Ulsan No. 14 National Expressway site. The expressway site is located near Burim-myeon of Uiryeong County in the South Gyeongsang Province of Korea and is primarily comprised of granite and pyrophyllite rocks. Four cross-hole seismic tests were conducted around the start and ends of the Burim 2 and Burim 3 tunnels (i.e., TB3-TB2, TB9-TB8, TB12-TB11 TB16-TB18). The features and conditions of the crosshole test site are shown in Fig. 12.

Rock mass classification was performed using the Q-system and RMR system along the depth of each borehole. The Q-values with depth are estimated based on the cross-hole seismic wave velocity data using the Q-value-shear wave velocity relationship equations in Fig. 10(c), as shown in Fig. 13. The corresponding range of shear wave velocity values from the confidence ellipses in Fig. 11 are also plotted with actual on-site Q-value measurements. The estimated Q-values agree well with the site measurements for all four cross-hole seismic tests and show improved correlations with increased stress. While the estimated Q-values may not be directly equal to the site-measured Q-values, the general range of probabilistic Q-values determined from the confidence ellipses show a similar

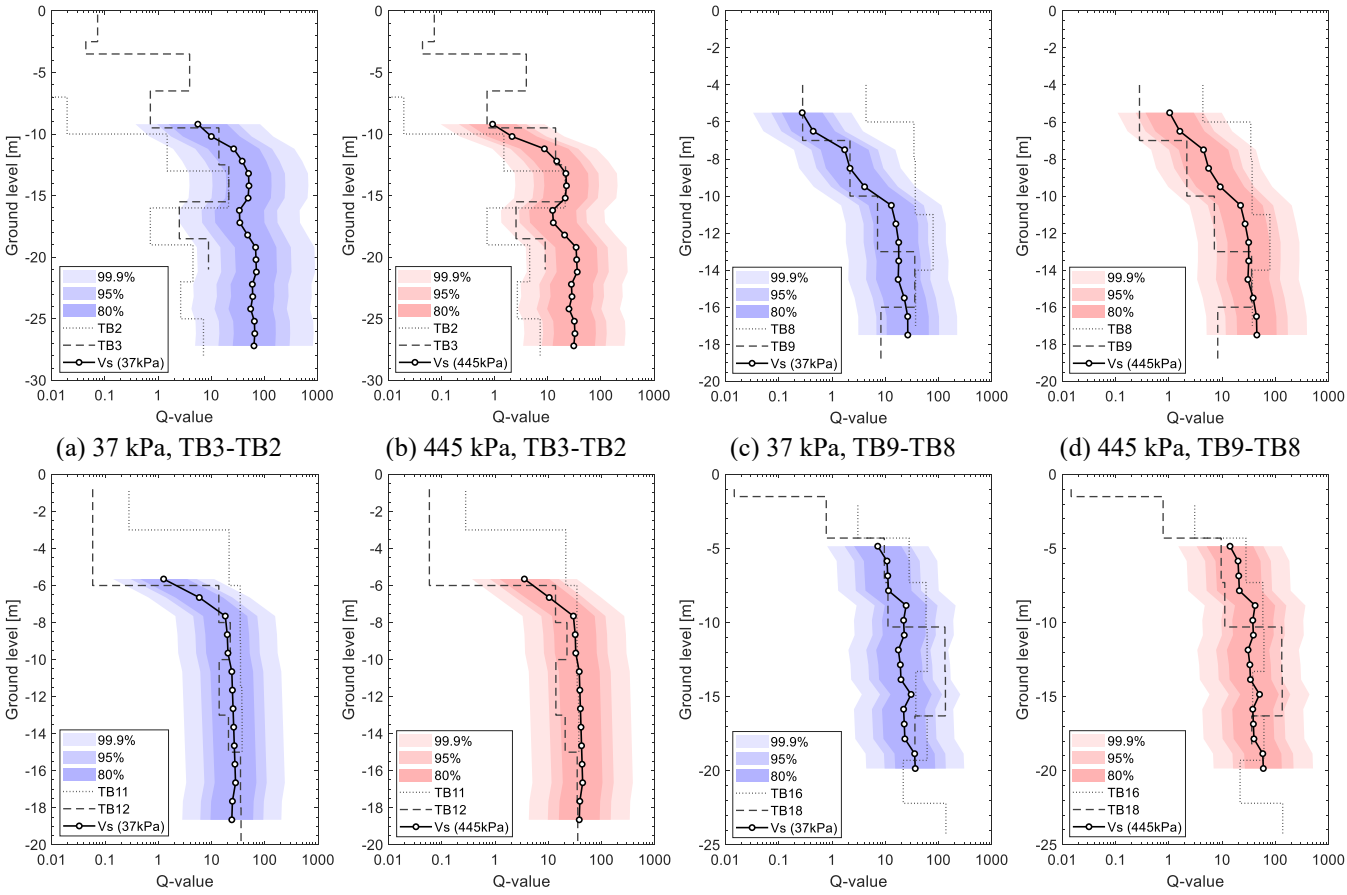

(a) 37 kPa, TB3-TB2 (b) 445 kPa, TB3-TB2 (c) 37 kPa, TB9-TB8 (d) 445 kPa, TB9-TB8

(e) 37 kPa, TB11-TB12 (f) 445 kPa, TB11-TB12 (g) 37 kPa, TB18-TB16 (h) 445 kPa, TB18-TB16

Fig. 13 Comparison between field measurements and Q-value estimations from crosshole seismic test

trend with the site measurements and the fluctuations in the Q-value with depth are well represented. The improved correlations for the 445 kPa estimations compared to the 37 kPa estimations highlight the importance of stress considerations in wave-based estimates of rock mass characteristics.

The limitations of the wave velocity-based Q-value estimations are apparent. The Q-value estimations and their accuracy depend on the extent to which the field-measured wave velocities portray the measured Q-value. The estimations can provide erroneous interpretations of the rock mass for areas having significant discrepancies between the measured wave velocity and rock quality (e.g., weak rock zones having high wave velocity). The laboratory-based wave velocity of rocks also differs from that of in-situ measurements and a wave velocity ratio between field and laboratory measured wave velocities can be adopted (Nourani *et al*. 2017). In addition, a single value of wave velocity is not enough to fully characterize the rock mass conditions accurately. Even with the confidence ellipses, the proposed relationship displays a wide range of Q-values for a single wave velocity value. Despite these limitations, the suggested relationships are based on the most probable outcomes according to the field data, and the Q-value estimate displays a generally good fit with actual Q-value measurements. Further consideration of stress anisotropy, the effects of groundwater, and site conditions such as the type of construction, type of rock, seismic survey method, and proper consideration of the site-specific environmental conditions can be considered to improve the accuracy and applicability of the suggested method. The Q-value-wave velocity relationships suggested in this study can be used to estimate rock mass characteristics when no coring or visible data are available.

7. Conclusions

In this study, a quantitative relationship between the Q-value and shear wave velocity was suggested by considering wave propagations in equivalent continuum jointed rock masses. The individual Q-system parameters were correlated with the stress-dependent shear wave velocities in jointed rocks using the QSRC test. A numerical model of the QSRC test specimen was replicated in the 3DEC, and the relationship between the shear wave velocity and joint set number, J_n, was investigated. Shear wave velocity data from previous studies were adapted to correlate the joint roughness, J_r, and the joint alteration, J_a, parameters with the shear wave velocity. The shear wave velocities were normalized into multiplication factors based on the reference wave velocities that corresponded to a single set of clean-cut, planar smooth joints having no joint fill. The Q-value-shear wave velocity relationship was

obtained from the relationships between individual Q-system parameters and shear wave velocity. The relationship was improved through probabilistic analysis to remove unrealistic combinations of Q-system parameters and to decrease data scatter. Confidence ellipses were calculated to provide a probabilistic range of Q-values for a given wave velocity. Field applications were performed based on cross-hole seismic test data to verify the applicability, reliability, and accuracy of the suggested relationship. The deduced Q-value-shear wave velocity relationship agreed well with previously noted relationships, further highlighting the importance of stress considerations in jointed rock masses. While the deduced probabilistic relationships in this study do not provide a universal method that can accurately correlate the wave velocity with the Q-value, it provides a probabilistic estimation of rock mass classification when conventional observations are impossible. The suggested relationships can be an effective tool for estimating and classifying in-situ rock masses based on seismic survey data when coupled with traditional site investigation methods.

Acknowledgment

This research was supported by the Institute for Korea Spent Nuclear Fuel (iKSNF) and the National Research Foundation of Korea (NRF) grant funded by the Korea Ministry of Science and ICT (MSIT) (2017R1A5A 1014883 and 2021M2E1A1085193).

References

Agliardi, F., Sapigni, M. and Crosta, G.B. (2016), "Rock mass characterization by high-resolution sonic and GSI borehole logging", *Rock Mech. Rock Eng.*, **49**(11), 4303-4318. https://doi.org/10.1007/s00603-016-1025-x.

Bandis, S.C., Lumsden, A.C. and Barton, N.R. (1983), "Fundamentals of rock joint deformation", *Int. J. Rock Mech. Min. Sci.*, **20**(6), 249-268. https://doi.org/10.1016/0148-9062(83)90595-8.

Barton, N. (1987), *Predicting the Behaviour of Underground Openings in Rocks*, Manuel Rocha Memorial Lecture, Lisbon, NGI Publication.

Barton, N. (2002), "Some new Q-value correlations to assist in site characterisation and tunnel design", *Int. J. Rock. Mech. Min. Sci.*, **39**(2), 185-216. https://doi.org/10.1016/S1365-1609(02)00011-4.

Barton, N. (2006), *Rock Quality, Seismic Velocity, Attenuation and Anisotropy*, CRC Press.

Barton, N., Lien, R. and Lunde, J. (1974), "Engineering classification of rock masses for the design of tunnel support", *Rock Mech.*, **6**(4), 189-236. https://doi.org/10.1007/BF01239496.

Bednarek, L. and Majcherczyk, T. (2020), "An analysis of rock mass characteristics which influence the choice of support", *Geomech. Eng.*, **21**(4), 371-377. https://doi.org/10.12989/gae.2020.21.4.371.

Bery, A.A. and Rosli, S. (2012), "Correlation of seismic P-wave velocities with engineering parameters (N value and rock quality) for tropical environmental study", *Int. J. Geosci.*, **3**(4), 749-757. https://doi.org/10.4236/ijg.2012.34075.

Bieniawski, Z.T. (1973), "Engineering classification of jointed rock masses", *Civil Eng. Sivil. Ing.*, **1973**(12), 335-343.

Cai, J. and Zhao, J. (2000), "Effects of multiple parallel fractures on apparent attenuation of stress waves in rock masses", *Int. J. Rock Mech. Min. Sci.*, **37**(4), 661-682. https://doi.org/10.1016/S1365-1609(00)00013-7.

Carter, T.G. (2010), "Applicability of classifications for tunnelling-valuable for improving insight, but problematic for contractual support definition or final design", *Proc. WTC.*, Vancouver, Paper 00401, Session 6c, 8.

Cha, M., Cho, G.C. and Santamarina, J.C. (2009), "Long-wavelength P-wave and S-wave propagation in jointed rock masses", *Geophys.*, **74**(5), E205-E214. https://doi.org/10.1190/1.3196240.

Cha, Y.H., Kang, J.S. and Jo, C.H. (2006), "Application of linear-array microtremor surveys for rock mass classification in urban tunnel design", *Expl. Geophys.*, **37**(1), 108-113. https://doi.org/10.1071/EG06108.

Chai, S., Li, J., Zhang, Q., Li, H. and Li, N. (2016), "Stress wave propagation across a rock mass with two non-parallel joints", *Rock Mech. Rock. Eng.*, **49**(10), 4023-4032. https://doi.org/10.1007/s00603-016-1068-z.

Chong, S.H., Kim, J.W. and Cho, G.C. (2014), "Rock mass dynamic test apparatus for estimating the strain-dependent dynamic properties of jointed rock masses", *Geotech. Test. J.*, **37**(2), 311-318. https://doi.org/10.1520/GTJ20120127.

Chong, S.H., Kim, J.W., Cho, G.C. and Song, K.I. (2020), "Preliminary numerical study on long-wavelength wave propagation in a jointed rock mass", *Geomech. Eng.*, **21**(3), 227-236. https://doi.org/10.12989/gae.2020.21.3.227.

Chong, S.H., Song, K.I. and Cho, G.C. (2021), "Development of equivalent stress-and strain-dependent model for jointed rock mass and its application to underground structure", *KSCE J. Civil Eng.*, **25**(12), 4887-4896. https://doi.org/10.1007/s12205-021-0616-6.

Cook, N.G. (1992), "Natural joints in rock: mechanical, hydraulic and seismic behaviour and properties under normal stress", *Int. J. Rock Mech. Min. Sci.*, **29**(3), 198-223. https://doi.org/10.1016/0148-9062(92)93656-5.

Deere, D.U. (1963), "Technical description of rock cores for engineering purpose", *Rock Mech. Eng. Geol.*, **1**(1), 17-22.

Edelbro, C., Sjöberg, J. and Nordlund, E. (2007), "A quantitative comparison of strength criteria for hard rock masses", *Tunn. Undergr. Space Technol.*, **22**(1), 57-68. https://doi.org/10.1016/j.tust.2006.02.003.

El-Naqa, A. (1996), "Assessment of geomechanical characterization of a rock mass using a seismic geophysical technique", *Geotech. Geol. Eng.*, **14**(4), 291-305. https://doi.org/10.1007/BF00421945.

Fratta, D. and Santamarina, J. (2002), "Shear wave propagation in jointed rock: State of stress", *Géotechnique*, **52**(7), 495-505. https://doi.org/10.1680/geot.2002.52.7.495.

Gong, L., Nemcik, J. and Ren, T. (2018), "Numerical simulation of the shear behavior of rock joints filled with unsaturated soil", *Int. J. Geomech.*, **18**(9), 04018112. http://doi.org/10.1061/(ASCE)GM.1943-5622.0001253.

Hong, C.H., Ryu, H.H., Oh, T.M. and Cho, G.C. (2020), "Probabilistic rock mass rating estimation using electrical resistivity", *KSCE J. Civil Eng.*, **24**, 2224-2231. https://doi.org/10.1007/s12205-020-1315-4.

Isik, N.S., Doyuran, V. and Ulusay, R. (2008), "Assessment of deformation modulus of weak rock masses from pressuremeter tests and seismic surveys", *Bull. Eng. Geol. Environ.*, **67**(3), 293-304. https://doi.org/10.1007/s10064-008-0163-0.

Itasca, C. (2013), 3DEC, Software, Version 5.0, Minneapolis.

Kahraman, S. (2002), "The effects of fracture roughness on P-wave velocity", *Eng. Geol.*, **63**(3-4), 347-350. https://doi.org/10.1016/S0013-7952(01)00089-8.

Kianpour, M., Aghda, S.M.F. and Talkhablou, M. (2020), "Classification of limestone rock masses using laboratory and field P-wave velocity by ArcGIS fuzzy overlay (AFO) (case study: five dam sites in Zagros Mountains, Western Iran)", *Geotech. Geol. Eng*., **38**(1), 631-650. https://doi.org/10.1007/s10706-019-01052-3.

Kim, J.W., Chong, S.H. and Cho, G.C. (2021), "Effects of gouge fill on elastic wave propagation in equivalent continuum jointed rock mass", *Mater.*, **14**(12), 3173. https://doi.org/10.3390/ma14123173.

Kim, J.W., Chong, S.H. and Cho, G.C. (2018), "Experimental characterization of stress-and strain-dependent stiffness in grouted rock masses", *Mater.*, **11**(4), 524. https://doi.org/10.3390/ma11040524.

Kolsky, H. (1963), *Stress Waves in Solids*, Vol. 1098, Courier Corporation, Chelmsford, MA, USA.

Leucci, G. and De Giorgi, L. (2006), "Experimental studies on the effects of fracture on the P and S wave velocity propagation in sedimentary rock ("Calcarenite del Salento")", *Eng. Geol.*, **84**(3-4), 130-142. https://doi.org/10.1016/j.enggeo.2005.12.004.

Li, J., Li, H., Jiao, Y., Liu, Y., Xia, X. and Yu, C. (2014), "Analysis for oblique wave propagation across filled joints based on thin-layer interface model", *J. Appl. Geophys*., **102**, 39-46. https://doi.org/10.1016/j.jappgeo.2013.11.014.

Li, J., Ma, G. and Zhao, J. (2010), "An equivalent viscoelastic model for rock mass with parallel joints", *J. Geophys. Res. Solid Earth*., **115**(B3), 1. https://doi.org/10.1029/2008JB006241.

Mohd-Nordin, M.M., Song, K.I., Cho, G.C. and Mohamed, Z. (2014), "Long-wavelength elastic wave propagation across naturally fractured rock masses", *Rock. Mech. Rock. Eng*., **47**(2), 561-573. https://doi.org/10.1007/s00603-013-0448-x.

NGI (2013), *Using the Q-System-Rock Mass Classification and Support Design*, NGI Publication, Oslo, Norway 54 p.

Nourani, M.H., Moghadder, M.T. and Safari, M. (2017), "Classification and assessment of rock mass parameters in Choghart iron mine using P-wave velocity", *J. Rock Mech. Geotech. Eng*., **9**(2), 318-328. https://doi.org/10.1016/j.jrmge.2016.11.006.

Palmström, A. (1996), "Characterizing rock masses by the RMi for use in practical rock engineering: Part 1: The development of the Rock Mass index (RMi)", *Tunn. Undergr. Space Technol.*, **11**(2), 175-188. https://doi.org/10.1016/0886-7798(96)00015-6.

Perino, A., Zhu, J., Li, J., Barla, G. and Zhao, J. (2010), "Theoretical methods for wave propagation across jointed rock masses", *Rock. Mech. Rock. Eng*., **43**(6), 799-809. https://doi.org/10.1007/s00603-010-0114-5.

Robertsson, J.O., Blanch, J.O. and Symes, W.W. (1994), "Viscoelastic finite-difference modeling", *Geophysics*., **59**(9), 1444-1456. https://doi.org/10.1190/1.1443701.

Ryu, H.H., Joo, G.W., Cho, G.C., Kim, K.Y. and Lim, Y.D. (2013), "Probabilistic rock mass classification using electrical resistivity-Theoretical approach of relationship between RMR and electrical resistivity", *J. Korean Tunn Undergr Sp*., **15**(2), 97-111. https://doi.org/10.9711/KTAJ.2013.15.2.097.

Ryu, H.H., Oh, T.M., Cho, G.C., Kim, K.Y., Lee, K.R. and Lee, D.S. (2014), "Probabilistic relationship between Q-value and electrical resistivity", *KSCE J. Civil Eng.*, **18**(3), 780-786. https://doi.org/10.1007/s12205-014-0339-z.

Salaamah, A.F., Fathani, T.F. and Wilopo, W. (2018), "Correlation of P-wave velocity with rock quality designation (RQD) in volcanic rocks", *J. Appl. Geol.*, **3**(2), 62-72. http://doi.org/10.22146/jag.48594.

Schoenberg, M. and Muir, F. (1989), "A calculus for finely layered anisotropic media", *Geophys*., **54**(5), 581-589. https://doi.org/10.1190/1.1442685.

Sebastian, R. and Sitharam, T.G. (2018), "Resonant column tests and nonlinear elasticity in simulated rocks", *Rock Mech. Rock Eng.*, **51**(1), 155-172. https://doi.org/10.1007/s00603-017-1308-x.

Sjøgren, B., Øfsthus, A. and Sandberg, J. (1979), "Seismic classification of rock mass qualities", *Geophys. Prospect*., **27**(2), 409-442. https://doi.org/10.1111/j.1365-2478.1979.tb00977.x.

Wyllie, M.R.J., Gregory, A.R. and Gardner, G.H.F. (1958), "An experimental investigation of factors affecting elastic wave velocities in porous media", *Geophys.*, **23**(3), 459-493. https://doi.org/10.1190/1.1438493.

Zerwer, A., Cascante, G. and Hutchinson, J. (2002), "Parameter estimation in finite element simulations of Rayleigh waves", *J Geotech. Geoenviron.*, **128**(3), 250-261. https://doi.org/10.1061/(ASCE)1090-0241(2002)128:3(250).

Zhao, X., Zhao, J., Cai, J. and Hefny, A.M. (2008), "UDEC modelling on wave propagation across fractured rock masses", *Comput. Geotech*., **35**(1), 97-104. https://doi.org/10.1016/j.compgeo.2007.01.001.

Zhao, Z., Jing, H., Shi, X., Yang, L., Yin, Q. and Gao, Y. (2021), "Study on bearing characteristic of rock mass with different structures: Physical modeling", *Geomech. Eng.*, **25**(3), 179-194. https://doi.org/10.12989/gae.2021.25.3.179.

Zhou, J. and Yang, X.A. (2021), "Deformation behavior analysis of tunnels opened in various rock mass grades conditions in China", *Geomech. Eng.*, **26**(2), 191-204. https://doi.org/10.12989/gae.2021.26.2.191.

Zhu, J., Deng, X., Zhao, X. and Zhao, J. (2013), "A numerical study on wave transmission across multiple intersecting joint sets in rock masses with UDEC", *Rock. Mech. Rock. Eng*., **46**(6), 1429-1442. https://doi.org/10.1007/s00603-012-0352-9.

IC